MECHANICAL CHARACTERIZATION OF POLYVINIL BUTYRAL FROM STATIC AND MODAL TESTS ON LAMINATED GLASS BEAMS

M.L. Aenlle, A. Noriega, F. Pelayo*

Department of Construction and Manufacturing Engineering, University of Oviedo, Campus de Gijón, Zona Oeste, Edificio 7, 33203, Gijón, Spain.

*corresponding author; E-mail: fernandezpelayo@uniovi.es

Tel: +34985181932

ABSTRACT

Polyvinyl butyral (PVB) is the polymeric interlayer material most used in laminated glass elements. As other used interlayers, the PVB mechanical behaviour is viscoelastic. Therefore, its mechanical characterization can be carried out by static (creep and relaxation) or dynamic tests in a dynamic mechanical analyzer (DMA). However, the PVB layers constrained in laminated glass elements are subject to high temperature and pressure conditions in an autoclave during the manufacturing process, which can affect to the mechanical properties of the interlayer. In this paper, the mechanical properties of PVB constrained in laminated glass beams have been determined by static and dynamic tests on laminated glass beams with different boundary conditions and at different temperatures. The estimated curves are compared with those obtained by testing free PVB specimens in a DMA.

Keywords: Polymer composites; Inverse characterization, laminated elements, viscoelasticity; modelling.

1 INTRODUCTION

Laminated glass elements are nowadays used in many mechanical and structural applications due to their advantages with respect to standard monolithic glass, such as vibration and noise

isolation, light transmittance, UV protection, safety improvement, impact resistance, etc. Laminated glass elements consist of two or more layers of monolithic glass with one or more polymer interlayers which present, in general, a viscoelastic behavior [1, 2, 3, 4]. Polyvinyl Butyral (PVB) is the most used interlayer material and it is commercialized in thicknesses of 0.38 mm or a multiple of this value (0.76 mm, 1.12 mm, 1.52 mm). The adherence of the glass and PVB layers is provided subjecting the shaped laminate to high temperature and pressure conditions in an autoclave.

As the tensile modulus of the PVB is far less in comparison with that corresponding to glass, significant transverse shear appears in the viscoelastic layer [1-10] and the degree of coupling depends upon the shear stiffness of the polymeric interlayer. Moreover, in laminated glass elements the interlayer carries transverse shear stress but the longitudinal stresses are negligible, which means that the behavior of the interlayer is commonly modelled considering only the shear modulus [1-10].

PVB is usually characterized as linear-viscoelastic [11, 12, 13], i.e. its mechanical properties are dependent of the load application time and the temperature working conditions [11, 12, 13]. This time and temperature dependence implies that the experimental mechanical characterization has to be carried out using a large number of assays in order to cover all the material working conditions. However, PVB can be considered a simply thermo-rheological material [11, 12, 13] and both variables (time and temperature) can be related through the Time–Temperature Superposition (TTS) principle [14, 15, 16]. A series of stretch time experiments at different temperatures can be shifted to a reference temperature in order to obtain a broad-band time master curve at the corresponding reference temperature.

The mechanical properties of a polymer with viscoelastic behavior can be determined using a Dynamic Mechanical Analyser (DMA). The mechanical properties in time domain are obtained from static creep or relaxation tests at different temperatures. The complex viscoelastic modulus (frequency domain) is determined by applying a sinusoidal stress or strain history. This test is repeated over a wide range of temperatures and frequencies (temperature sweep or frequency sweep) [12].

However, the tests and the analysis of the results must be carried out by personnel with experience in viscoelasticity because small details can have significant influence in the estimated mechanical properties. Moreover, both parameters relaxation modulus $E(t)$ and relaxation shear modulus $G(t)$ are needed in the finite element programs to fully define the

mechanical properties of polymeric materials. However, PVB is commercialized in very thin films and it is difficult to determine $G(t)$ from shear or torsional tests. In order to simplify the material characterization, some assumptions (constant volumetric modulus K ($= 2$ GPa in [17]), constant Poisson's ratio ν ($\nu = 0.49$ in [18], etc.) are usually considered to define the mechanical behaviour knowing only $E(t)$. All these reasons lead to different mechanical properties of PVB published in the scientific literature [17, 18, 19]. The mechanical properties of PVB determined by the authors testing PVB specimens in a DMA, were published in [18, 20] and the coefficients of the Prony series have been replicated in Table 1.

In the last years, authors have predicted the static response [21, 22] and the modal parameters [9, 21, 23, 24] of laminated glass beams and plates using the mechanical properties shown in Table 1 and validated by experimental results. The discrepancies in deflections, stresses and natural frequencies are within the range 0% -20%.

However, in the glass community is said that the mechanical properties of PVB change after the process in autoclave. This means that the PVB exhibits different behaviour when it is tested freely (not constrained in a laminate) or when it is tested in constrained conditions in laminated glass elements. However, to the author's knowledge studies investigating these effects have not been reported in the literature.

In this paper, a methodology to determine the shear modulus $G(t)$ and the complex shear modulus $G^*(\omega)$ of PVB, using the experimental response of laminated glass beams with PVB interlayer, is presented. On one hand, several static tests at different temperatures in simply supported laminated glass beams were performed in a climate chamber. From the experimental static deflection, the shear modulus $G(t)$ was estimated using the model developed by Galuppi and Royer-Carfagni [1]. On the other hand, the modal parameters of several free-fee laminated glass beams tested at different temperatures in a climate chamber, were estimated by operational modal analysis. The complex shear modulus $G^*(\omega)$ was estimated using the experimental modal parameters (natural frequencies and the damping ratios) and the model developed by Ross, Kerwin and Ungar (RKU) [5,6]. Then, the discrete values of $G(t)$ and $G^*(\omega)$ were fitted to a Generalized Maxwell model expressed in terms of Prony's series. Finally, the curve G(t) obtained with the proposed methodology is compared with that obtained by free-free testes in PVB specimens [18].

2 STATE OF THE ART

2.1 VISCOELASTIC BEHAVIOR

The mechanical behavior of a viscoelastic material can be established by relaxation or creep tests in time domain [11, 12, 13] or by dynamic tests (sweep frequency, sweep strain, etc.) in frequency domain [11, 12, 13].

The $E(t)$, is usually fitted with a generalized Maxwell model [11, 12, 13] which can be represented with Prony's series as:

$$E(t) = E_0\left(1 - \sum_{i=1}^{n} e_i + \sum_{i=1}^{n} e_i \cdot exp\left(-\frac{t}{\tau_{iE}}\right)\right) \quad (1)$$

where e_i and τ_{iE} are the Prony's series coefficients, n is the number of terms and E_0 is the instantaneous modulus.

In frequency domain, the complex tensile modulus, $E^*(\omega)$ is given by:

$$E^*(\omega) = E'(\omega) + i \cdot E''(\omega) = E'(\omega)(1 + i \cdot \eta\,(\omega)) \quad (2)$$

where superscript '*' indicates complex, ω represents the frequency, i is the imaginary unit, $E'\,(\omega)$ y $E''\,(\omega)$ are the storage and the loss tensile moduli, respectively, and

$$\eta\,(\omega) = \frac{E''(\omega)}{E'(\omega)} \quad (3)$$

is the loss factor that relates both moduli.

The storage $E'(\omega)$ and the loss $E''(\omega)$ moduli can also been expressed in terms of Prony's series as:

$$E'(\omega) = E_0\left(1 - \sum_{i=1}^{n} \mathrm{e_i} \ + \sum_{i=1}^{n} \frac{\tau_{iE}^2 \cdot \omega^2 \cdot e_i}{1 + \tau_{iE}^2 \cdot \omega^2}\right) \tag{4}$$

and

$$E''(\omega) = E_0\left(\sum_{i=1}^{n} \frac{\tau_{iE} \cdot \omega \ \cdot e_i}{1 + \tau_{iE}^2 \cdot \omega^2}\right) \tag{5}$$

The same procedure can be followed with the relaxation shear modulus $G(t)$:

$$G(t) = G_0 + \left(1 - \sum_{i=1}^{n} g_i - \sum_{i=1}^{n} g_i \cdot exp\left(-\frac{t}{\tau_{iG}}\right) \right) \tag{6}$$

And the storage and the loss shear moduli as:

$$G'(\omega) = G_0\left(1 - \sum_{i=1}^{n} \mathrm{e_i} \ + \sum_{i=1}^{n} \frac{\tau_{iG}^2 \cdot \omega^2 \cdot e_i}{1 + \tau_{iG}^2 \cdot \omega^2}\right) \tag{7}$$

$$G''(\omega) = G_0\left(\sum_{i=1}^{n} \frac{\tau_{iG} \cdot \omega \ \cdot e_i}{1 + \tau_{iG}^2 \cdot \omega^2}\right) \tag{8}$$

It is commonly assumed that [25]:

$$\tau_i = \tau_{iG} = \tau_{iE} \tag{9}$$

Due to the fact that polymers present temperature-dependent mechanical properties, the time–temperature superposition principle (TTS) [14, 15, 16] is commonly used to determine the mechanical properties of linear viscoelastic materials at different temperatures. In time domain,

the modulus at temperature, T_1, can be estimated by shifting in time the modulus at temperature T_0 using a shift factor, $a_T = a_T(T_0, T_1)$, i.e.:

$$E(t_0, T_0) = a_T\, E(t_1, T_1) \tag{10}$$

A similar process is followed in frequency domain. If the William, Landel and Ferry (WLF) model [26] is used to shift the curves, the shift factor, a_T, is expressed as:

$$\log(a_T) = -C_1 \frac{(T - T_0)}{C_2 + (T - T_0)} \tag{11}$$

Where C_1 and C_2 are constants of the model.

2.2 STATIC DEFLECTIONS OF LAMINATED GLASS BEAMS

Galuppi and Royer-Carfagni [1] derived an analytical expression to calculate the static deflection of a laminated glass beam composed of two glass layers and one polymeric interlayer (Fig 1), assuming that the deflection shape of the laminated glass beam coincides with that of a monolithic beam with the same loading and boundary conditions. The deflection $w(x)$ of the beam is expressed as:

$$w(x) = -\frac{q(x)}{EI_T \left(1 + \dfrac{Y_B}{1 + \dfrac{EH_1 t H_2}{G(H_1 + H_2)} \psi_B} \right)} \tag{12}$$

where

- Sub-index “S” indicates static,
- $q(x)$ is a shape function that takes the form of the elastic deflection of a monolithic beam with constant cross section under the same loading and boundary conditions as the laminated glass beam,
- H_1 and H_2 are the thickness of the glass layers,
- t is the thickness of the polymeric interlayer,
- E is the Young’s modulus of the glass layers,

- G is the shear modulus of the polymeric interlayer,
- Y_B is a geometric parameter given by:

$$Y_B = \frac{bH_1H_2}{I_T(H_1+H_2)}\left(t + \frac{H_1+H_2}{2}\right) \tag{13}$$

- $I_T = I_1 + I_2 = b\frac{H_1^3+H_2^3}{12}$ (14)

- And ψ_B is a constant parameter which depends on the boundary and loading conditions [1] and it can be calculated from the expression:

$$\psi_{B2} = \frac{\int_0^L \left(q''(x)\right)^2 dx}{\int_0^L \left(q'(x)\right)^2 dx} \tag{15}$$

The values for the most common boundary and loading conditions are reported in [26].

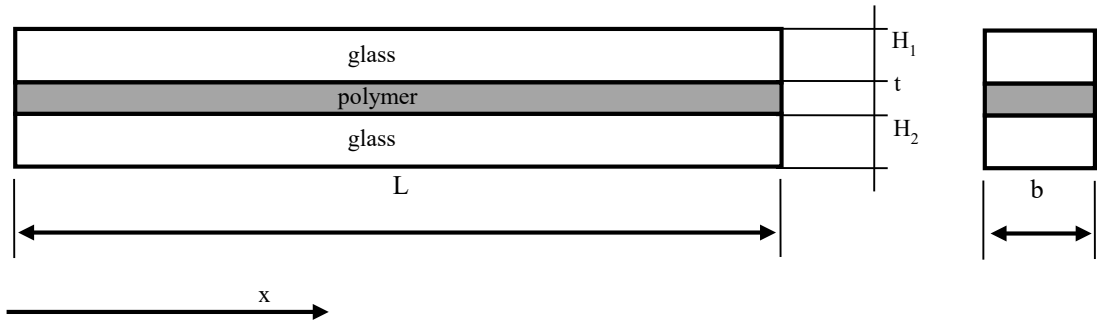

Figure 1: Geometry of a laminated glass beam

Due to the fact that PVB shows a viscoelastic behavior, a quasi-static analysis has to be performed to determine the deflection of a laminated glass beam. In order to simplify the calculations, the secant stiffness approximation [27] can be used. This technique consists of modelling the polymer as a linear elastic material, taking at each instant t its equivalent elastic modulus $G_t(t)$, i.e. the shear stress is a given by:

$$\tau(t) = G_t(t) \cdot \gamma(t) \tag{16}$$

where $\gamma(t)$ is the strain in the polymer and $G(t)$ is the shear modulus. The solution obtained under this assumption is known as Secant Stiffness Solution (SSS) [27]. This solution provides accurate results for constant (in time) static loadings [21, 27].

The deflection of a laminated glass beam using the model developed by Galuppi and Royer-Carfagni and the secant stiffness approximation, can be calculated using the expression:

$$w^{SSS}(x,t,T) = -\frac{q(x)}{EI_T\left(1+\dfrac{Y_B}{1+\dfrac{EH_1tH_2}{G(t,T)(H_1+H_2)}\psi_B}\right)} \tag{17}$$

Which is easily inferred from Eq. (12) considering $G = G(t,T)$.

2.3 MODAL PARAMETERS OF LAMINATED GLASS BEAMS

Ross, Kerwin, and Ungar [5, 6] developed a model (RKU model) for the flexural vibrations of sandwich elements considering the beam simply supported and assuming a flexural deformation spatially sinusoidal in shape. The model can be extended to other boundary conditions using appropriate wavenumbers [28] and it has been used by different authors to determine de mechanical behavior of viscoelastic materials [9, 23].

If the RKU model is used, the natural frequencies ω and the loss factors η of a laminated glass beam can be estimated with the equation:

$$\omega^{*2} = \omega^2(1+i\cdot\eta) = k_I^4\frac{EI^*(\omega)}{\overline{m}} \tag{18}$$

where:

- k_I is the wavenumber,
- $EI^*(\omega)$ is the complex stiffness given by:

$$EI^*(\omega) = EI_{T2}\left(1 + \frac{Y_{B2}}{1 + \frac{EH_1tH_2\,k_I^2}{G^*(\omega,T)(H_1+H_2)}}\right) \quad (19)$$

- $G^*(\omega,T)$ is the complex shear modulus,
- $\overline{m}$ is the mass per unit length:

$$\overline{m} = \rho_G(H_1 + H_2) + \rho_t \cdot t \quad (20)$$

- and ρ_G and ρ_t are the mass density of the glass layers and the polymeric interlayer, respectively.

2.4 RELAXATION TESTS IN FREE SPECIMENS

In a previous work [18, 20], the viscoelastic properties of the PVB were determined from tensile relaxation tests carried out in a DMA RSA3 by T.A. Instruments [29]. The material used in the experiments was standard PVB (Polyvinyl butyral) being the geometry of specimens: length 25 mm, width 5 mm and thickness 0.38 mm. Fifteen tensile relaxation tests were conducted at different temperatures from -15^oC to 50^oC at a constant strain $\varepsilon_0 = 1\%$ for all the tests.

The experimental master curve $E(t)$ for a reference temperature $T = 20^oC$ and the viscoelastic fitted model using 13 terms in the Prony series expression (R-square 0.99943) are presented in Fig . 2. The master curve at 20^oC was obtained by shifting the master curve at $T_s = 50^oC$ using the WLF model and the constants calculated $C_1 = 12.601$ and $C_2 = 74.76$ [20]. The coefficients of the Prony series are presented in Table 1, the instantaneous modulus being $E_0 = 1.2403$ GPa.

The shear modulus $G(t)$ was derived from $E(t)$ assuming a constant Poisson's ratio ($= 0.49$) . This is equivalent to assume that the material is quasi-incompressible.

Table 1. Prony series coefficients for PVB

e_i	τ_i [s]
2.342151953E-01	2.36600000000000E-07

2.137793134E-01	2.26430000000000E-06
1.745500419E-01	2.16668000000000E-05
1.195345045E-01	2.07327300000000E-04
1.362133454E-01	1.98389580000000E-03
6.840656310E-02	1.89837195000000E-02
4.143944180E-02	1.81653498300000E-01
7.251952800E-03	1.73822593210000E+00
2.825459600E-03	1.66329270788000E+01
2.712854000E-04	1.59158978189400E+02
4.293523000E-04	1.52297789909670E+03
9.804730000E-05	1.45732380763177E+04
5.274937000E-04	1.39449999999999E+05

Once the relaxation modulus of the material is known in terms of Prony coefficients, (e_i, τ_i), the storage modulus $E'(\omega)$ and the loss modulus $E''(\omega)$ can be obtained with Eqs. (4) and (5).

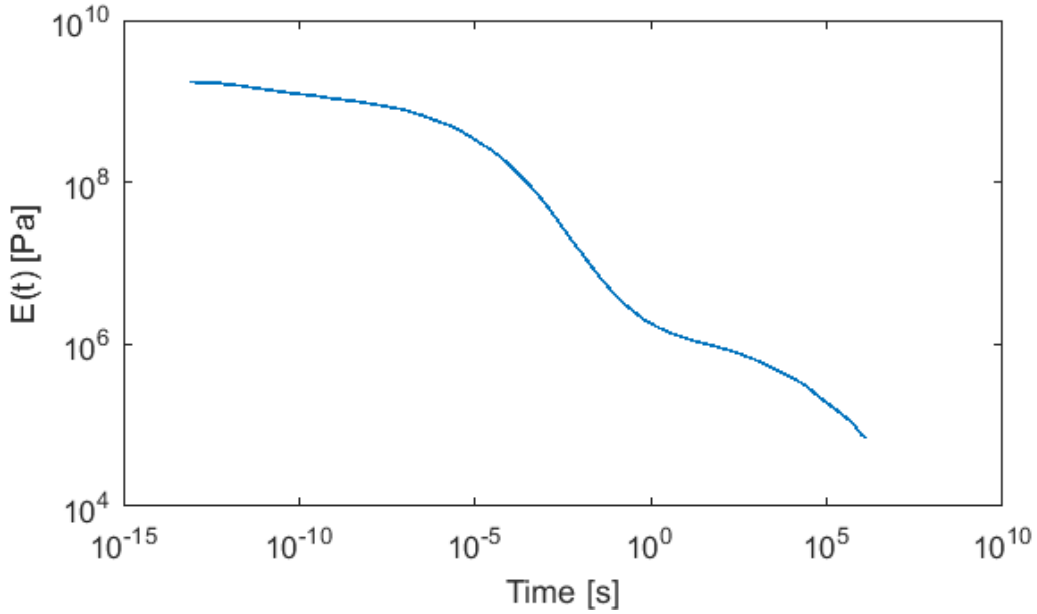

Figure 2. Relaxation curve for free PVB obtained by TTS.

3 STATIC TESTS

Two laminated glass beams with the geometrical data shown in Table 2, were subject to a static concentrated loading at the mid-point of the beam in simply-supported conditions. The tests were performed in a climate chamber at 25ºC, 30ºC, 35ºC and 40ºC, respectively (see Fig. 3), for approximately 24 hours. The deflection $w\left(x=\frac{L}{2},t,T\right)_{exp}$ at mid-span was measured with a laser sensor.

If Eq. (17) is particularized for a simply supported beam subject to a concentrated loading at the mid-point of the beam and the deflection $w^{SSS}\left(x=\frac{L}{2}t,T\right)$ is substituted by the corresponding experimental deflection $\left(x=\frac{L}{2},t,T\right)_{exp}$, it results in:

$$w\left(x=\frac{L}{2},t,T\right)_{exp}=-\frac{PL^3}{48\cdot EI_T\left(1+\frac{Y_B}{1+\frac{EH_1tH_2}{G(t,T)(H_1+H_2)}\psi_B}\right)} \tag{21}$$

where the shear modulus $G(t,T)$ is the only unknown. A Young's modulus $E=72\ GPa$ has been considered for the glass layers, whereas the parameter $\psi_B=\frac{10}{L^2}$ was taken from [26] .

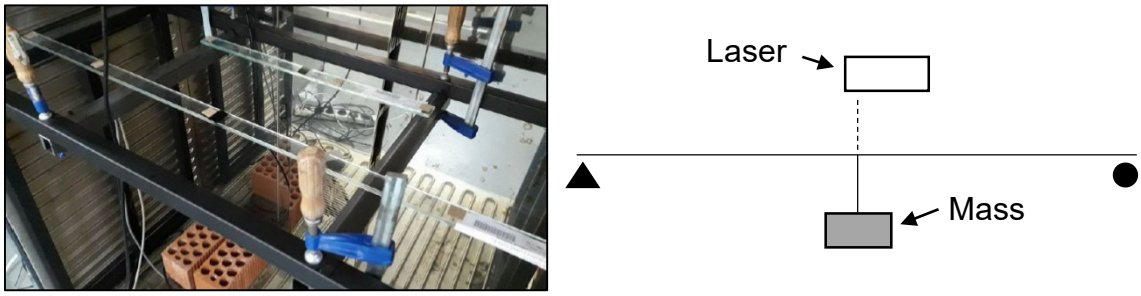

Figure 3. Test setup for the static tests.

The shear modulus $G(t,T)$ at 35ºC, obtained from both beams ($L = 1\,m$ and $L = 0.5\,m$ is presented in Fig. 4.

Table 2. Geometry of the laminated glass beams and magnitude of the loadings.

Beam	H_1 (mm)	H_2 (mm)	t (mm)	b (mm)	L (m)	P (N) 25ºC, 30ºC and 35ºC	P (N) at 40ºC
1	3.05	3.12	0.75	30	1	5	3
2	3.05	3.12	0.75	30	0.5	10	8

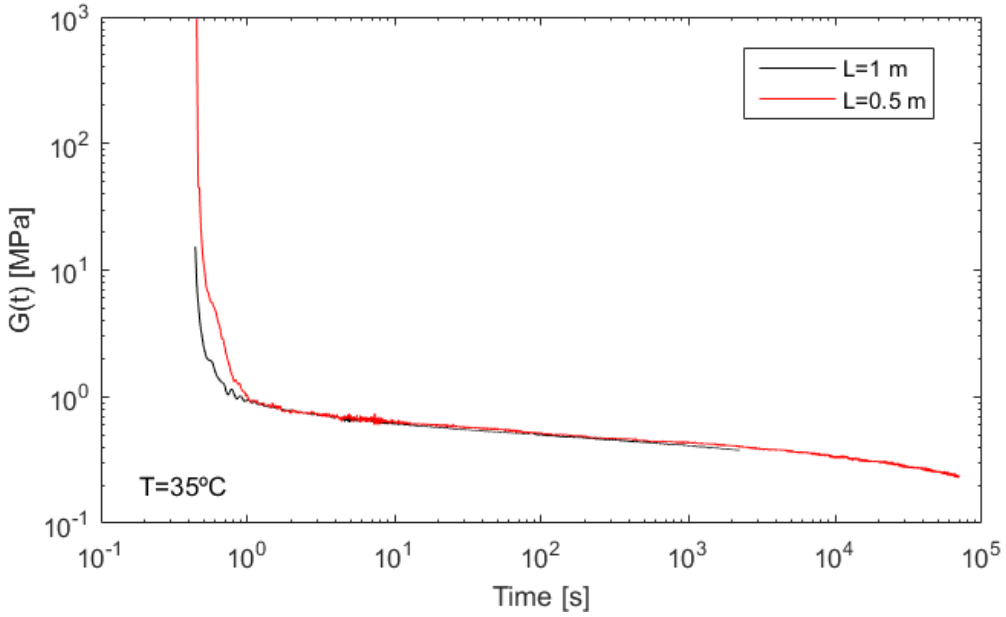

Figure 4. Shear modulus $G_t(t,T)$ at 35ºC from static tests.

4 OPERATIONAL MODAL TESTS

Several laminated glass beams with different geometries (see appendix) were tested in free-free boundary conditions in a climate chamber and the modal parameters corresponding to the first bending four modes were estimated with operational modal analysis [30].

The responses of the beams were measured using accelerometers with a sensitivity of 100 mV/g, uniformly distributed along the beams and recorded with a digital acquisition card. The beams were excited applying small hits randomly along their length and the responses were recorded for approximately 4 minutes using sampling frequencies in the range $1000 - 2000$ Hz. The modal tests were performed at temperatures from 11ºC to 50 ºC.

The modal parameters were estimated using both Frequency Domain Decomposition (EFDD) [30] and Stochastic Subspace iteration method (SSI) [30]. The experimental natural frequencies and damping ratios estimated with the EFDD technique are shown in the appendix. The SSI technique provides similar results and they are not presented in the paper.

If the mechanical properties of the glass and the geometric dimensions are known and the experimental natural frequencies ω_{exp} and loss factors η_{exp} are substituted in Eq. (18), the shear modulus $G^*(\omega, T)$ is the only unknown. The mechanical properties shown in Table 3 were considered for the glass and the PVB layers.

Table 3. Material properties for glass and PVB.

Glass		PVB		
E (Young's Modulus) [GPa]	ρ_G (Density) [kg/m^3]	ρ_t (Density) [kg/m^3]	C_1 (WLF: Tref=20ºC)	C_2 (WLF: Tref=20ºC)
72	2500	1046	12.60	74.46

The storage shear modulus $G'(\omega, T)$ and the loss factor $\eta(\omega, T)$ obtained with Eq. (18) are shown in Figs. (5) and (6), respectively. In order to facilitate the interpretation, the values corresponding to different temperatures have been shifted and the values presented in Figs. (5) and (6) correspond to a reference temperature $T_0 = 20^o$.

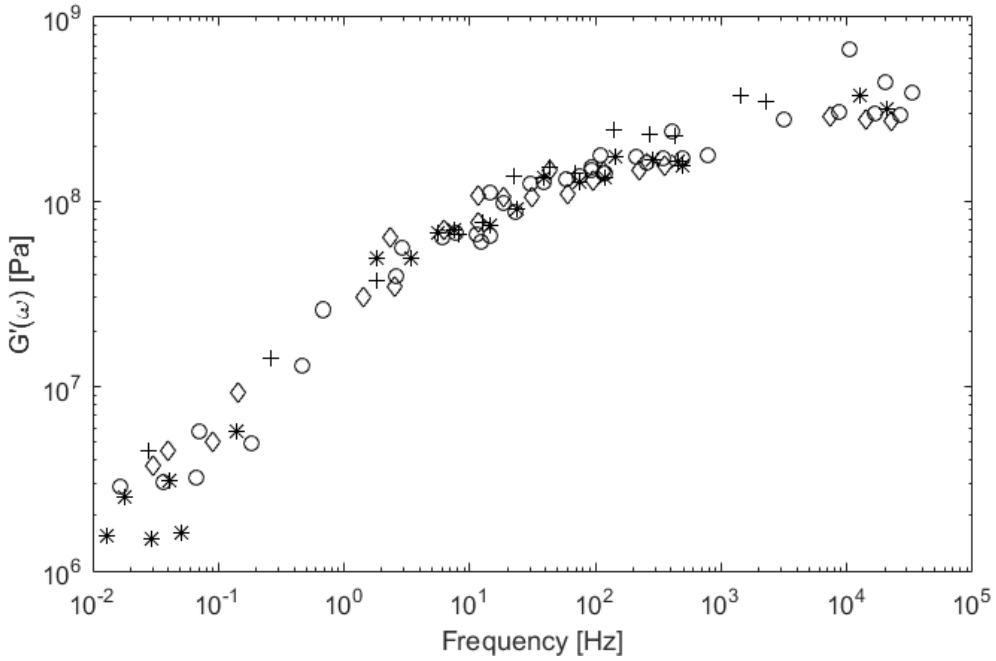

Figure 5. Storage shear modulus for the PVB obtained from the laminated glass beams with: '*' $t = 0.38\,mm$, 'o' $t = 0.76\,mm$, '♦' $t = 1.14\,mm$, '+' $t = 1.56\,mm$.

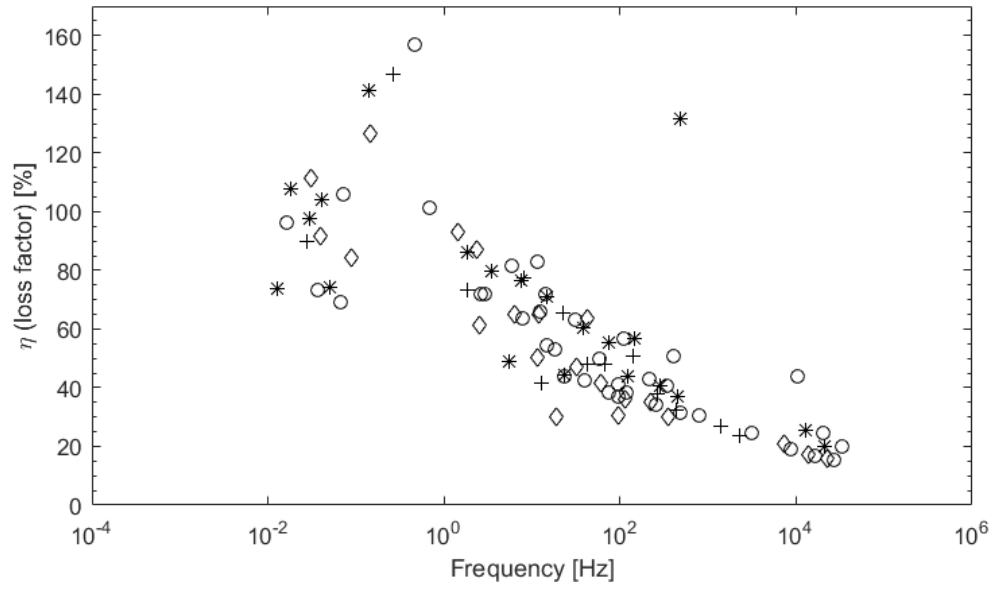

Figure 6. Loss factor η for the PVB obtained from the laminated glass beams with: '*' $t = 0.38\ mm$, 'o' $t = 0.76\ mm$, '♦' $t = 1.14\ mm$, '+' $t = 1.56\ mm$.

6 FITTING OF THE EXPERIMENTAL RESULTS

The experimental discrepancies results $G^*(\omega, T)$ were initially shifted to the reference temperature $T = 20^oC$ (see Figs. 5 and 6) using the WLF model with the constant parameters C_1 and C_2 shown in Table 3. It can be observed in Figs. 5 and 6 that the data shows a good trend so it was decided to keep these parameters. It is remarkable to mention that he parameters C_1 and C_2 presented in Table 3 for a reference temperature $T = 20^oC$, take the values $C_1 = 8.9932$ and $C_2 = 104.76$ for a reference temperature $T = 50^oC$, which are close to the universal constants $C_1 = 8.86$ and $C_2 = 101.6$ proposed by William, Landel and Ferry (WLF) [31], the errors being 1.5% and 3% for C_1 and C_2, respectively [18].

Moreover, the static data were shifted with the same constant parameters and then decimated in order to work with a reasonable number of points (Fig. 7).

From Eqs. (17) and (18), the shear relaxation modulus $G(t, T)$ and the complex shear modulus $G^*(\omega, T)$ are estimated. However, from the tensile relaxation tests carried out in a DTMA in free specimens, the parameters $E(t, T)$ and $E^*(\omega, T)$ are known. In order to compare both techniques, the tensile relaxation modulus was determined assuming a Poisson's ratio $\nu = 0.49$ [18], i.e. $E(t) \approx 3G(t)$, and the storage modulus as $E'(\omega) \approx 3G'(\omega)$.

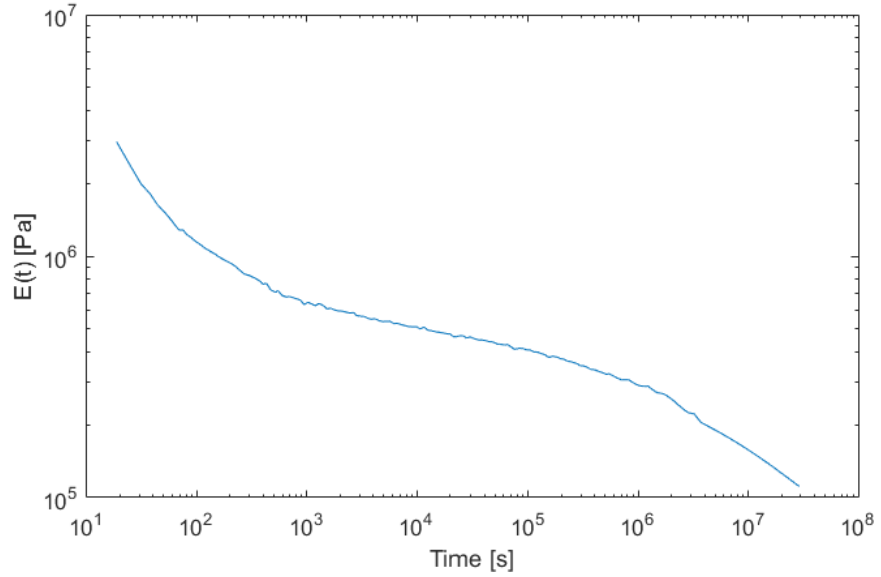

Figure 7. Relaxation modulus $E\,(t, T = 20ºC)$ from static tests.

The Ninomiya-Ferry algorithm [32] was used to convert data from frequency domain to time domain, obtaining that the frequency domain tests cover the following time domain range:

$$[t_{min}, t_{max}]_d = \left[\frac{1}{f_{max-exp}}, \frac{1}{f_{min-exp}}\right] = [3.0541 \cdot 10^{-5}, 77.8451]\ s \tag{22}$$

whereas the static tests cover the range:

$$[t_{min}, t_{max}]_s = [101, 29.5334 \times 10^6]\ s \tag{23}$$

Where sub-indexes ‘d’ and ‘s’ indicates data from dynamic and static tests, respectively.

Due to fact that there is no overlap between ranges given by Eqs. (22) and (23), the frequency domain data and the time domain data were analysed separately and then joined to obtain a Prony series covering a larger time range as:

$$\begin{aligned} &E\left(E_0, t, \tau_{id}, e_{id}, \tau_{js}, e_{js}\right) \\ &\quad = E_0\left(1 - \sum_{i=1}^{n_d} e_{id}\left(1 - \exp\left(-\frac{t}{\tau_{id}}\right)\right)\right. \\ &\quad \left. - \sum_{j=1}^{n_s} e_{js}\left(1 - \exp\left(-\frac{t}{\tau_{js}}\right)\right)\right) \end{aligned} \tag{24}$$

Where

- n_d is the number of terms of the Prony series used to fit the dynamic tests.
- n_s is the number of terms of the Prony series used to fit the static tests
- τ_{id} parameter τ_i obtained from the dynamic tests
- τ_{js} parameter τ_j obtained from the static tests
- e_{id} parameter e_i obtained from the dynamic tests
- e_{js} parameter e_j obtained from the static tests

6.1 DATA FROM MODAL TESTS (FREQUENCY DOMAIN)

The experimental storage modulus $E'_{exp}(\omega_k)$ obtained from the data shown in the appendix were fitted with Eqs. (4) and (5). The parameters e_{id} and τ_{di} were estimated minimizing the following error function $F(E_0, \tau_{id}, e_{id})$ which represents the error between the analytical model given by Eq. (5) and the experimental results, i.e.:

$$F(E_0, \boldsymbol{\tau_d}, \boldsymbol{e_d}) = \sum_{k=1}^{r} \Phi_k^2(\omega_k, E_0, \boldsymbol{\tau_d}, \boldsymbol{e_d}) \tag{25}$$

Where r is the number of experimental data and

$$\boldsymbol{\tau_d} = \left[\tau_{1d}, \tau_{2d}, \dots \dots . \tau_{n_d d}\right] \tag{26}$$

$$\boldsymbol{e_d} = \left[e_{1d}, e_{2d}, \dots \dots . e_{n_d d}\right] \tag{27}$$

$$\Phi_{\mathrm{k}}(E^0, \boldsymbol{\tau_d}, \boldsymbol{e_d}) = E'(\omega_k, E_0, \boldsymbol{\tau_d}, \boldsymbol{e_d}) - E'_{exp}(\omega_k) \tag{28}$$

$$E'(\omega_k, E_0, \boldsymbol{\tau_d}, \boldsymbol{e_d}) = E_0 \left(1 - \sum_{i=1}^{n_d} \mathrm{e_{id}} \; + \sum_{i=1}^{n_d} \frac{\tau_{id}^2 \cdot \omega_k^2 \cdot e_{id}}{1 + \tau_{id}^2 \cdot \omega_k^2} \right) \tag{29}$$

The problem focuses firstly on minimizing the quadratic error in the storage modulus and then checked if the error is also small in the loss factors. It has been done in this way because we have a high scatter in the loss factor obtained from the experimental tests. Moreover, it is well known that the RKU model does not provide a good accuracy in the estimation of the loss factor [9, 21, 22, 24]. However, the loss modulus $E''(\omega_k, \boldsymbol{\tau_d}, \boldsymbol{e_d})$ can be also added to the error function in order to consider both the real and the imaginary parts.

After several trials with different number of terms n_d , the best fit was obtained considering nine terms n_d to fit the generalized Maxwell model expressed in terms of Prony series. Moreover, an homogeneous distribution in the logarithmic scale was considered for the terms τ_{id} as follows:

$$\tau_{id-min} = \log_{10} \frac{1}{f_{max-exp}}$$

$$\tau_{id-max} = \log_{10} \frac{1}{f_{min-exp}} \tag{30}$$

$$\tau_{id} = \tau_{id-min} + \frac{\tau_{id-max} - \tau_{id-min}}{n+1} \cdot i \qquad i = 1,2, \ldots . . n_d$$

With these assumptions the only unknowns are the terms E_0 and $\boldsymbol{e_d}$.

The square error formulation used in Eq. (25) allows to use the gradient method, i.e.:

$$\nabla F(E^0, \boldsymbol{e_d}) = 2 \cdot \boldsymbol{\Phi^T} \cdot \boldsymbol{J}(\boldsymbol{\Phi}) \tag{31}$$

Where

$$\boldsymbol{\Phi} = [\Phi_1, \ldots \ldots \Phi_r]^T \tag{32}$$

And $\boldsymbol{J}(\boldsymbol{\Phi})$ is the Jacobian matrix given by:

$$\boldsymbol{J}(\boldsymbol{\Phi}) = \begin{bmatrix} \frac{\partial \Phi_1}{\partial E_0} & \frac{\partial \Phi_1}{\partial e_{1d}} & \cdots & \frac{\partial \Phi_1}{\partial e_{n_d d}} \\ \vdots & \vdots & \ddots & \vdots \\ \frac{\partial \Phi_r}{\partial E_0} & \frac{\partial \Phi_r}{\partial e_{1d}} & \cdots & \frac{\partial \Phi_r}{\partial e_{n_d d}} \end{bmatrix} \tag{33}$$

With:

$$\frac{\partial \Phi_j}{\partial E_0} = \left(1 - \sum_{i=1}^{n_d} \mathrm{e_{id}} \; + \sum_{i=1}^{n_d} \frac{\tau_{id}^2 \cdot \omega_j^2 \cdot e_{id}}{1 + \tau_{id}^2 \cdot \omega_j^2} \right) \tag{34}$$

and

$$\frac{\partial \Phi_j}{\partial e_{id}} = E_0 \left(-1 + \frac{\tau_{id}^2 \cdot \omega_j^2}{1 + \tau_{id}^2 \cdot \omega_j^2} \right) \tag{35}$$

The solution was addressed using the trust-region-reflective algorithm (implemented in the Matlab function lsqcurvefit [32]) considering the following constraints:

$$\begin{aligned} & E_0 \geq 0 \\ & e_{id} \geq 0 \quad \forall i \end{aligned} \tag{36}$$

And the initial values:

$$\begin{aligned} & E_0 = 1.2403 \; GPa \text{ (from [18])} \\ & e_{id} = 0.001 \end{aligned} \tag{37}$$

The Prony terms e_{id} and τ_{id} estimated minimizing Eq. (25) are presented in Table 4 whereas the parameter E_0 takes de value $E_0 = 1.0579 \; GPa$.

Table 4. Parameters of the Prony series from dynamic tests.

n_d	τ_{id}	e_{id}
1	1.3351e-4	0.5185
2	5.8368e-4	0.0121
3	0.0026	0.1445
4	0.0112	0.1700
5	0.0488	0.0330
6	0.2132	0.1011

7	0.9318	0.0093
8	4.0734	0.0058
9	17.8072	0.0015

6.2 DATA FROM STATIC TESTS (TIME DOMAIN)

The values $G(t,T)$ estimated from the experimental static testes were fitted with Eq. (24). The parameters e_{js} and τ_{js} were determined minimizing the error function $F_s(\tau_{js}, e_{js})$ which represents the error between the analytical model given by Eq. (1) and the experimental results:

$$F_s(\boldsymbol{\tau_s}, \boldsymbol{e_s}) = \sum_{k=1}^{s} \boldsymbol{\Psi_k^2}(t_k, \boldsymbol{\tau_s}, \boldsymbol{e_s}) \tag{38}$$

Where 's' is the number of experimental data considered in the analysis and

$$\boldsymbol{\tau_s} = [\tau_{1s}, \tau_{2s}, \ldots\ldots \tau_{n_s s}] \tag{39}$$

$$\boldsymbol{e_s} = [e_{1s}, e_{2s}, \ldots\ldots e_{n_s s}] \tag{40}$$

$$\Psi_k(t_k, \boldsymbol{\tau_s}, \boldsymbol{e_s}) = E(t_k, \boldsymbol{\tau_s}, \boldsymbol{e_s}) - E_{exp}(t_k) \tag{41}$$

After several trials with different number of terms n_s , the best fit was obtained considering seven terms n_s for the Prony series and an homogeneous distribution in the logarithmic scale was considered for the terms τ_{js} as follows:

$$\begin{aligned} &\tau_{js-min} = \log_{10} 101 \\ &\tau_{js-max} = \log_{10} 29.5334 \times 10^6 \\ &\tau_{js} = \tau_{js-min} + \frac{\tau_{js-max} - \tau_{js-min}}{n_s + 1} \cdot j \qquad j = 1,2, \ldots\ldots n_s \end{aligned} \tag{42}$$

Again, the square error formulation used in Eq. (38) allows to use the gradient method, i.e.:

$$\nabla F_s(e_{js}) = 2 \cdot \boldsymbol{\Psi^T} \cdot \boldsymbol{J}(\boldsymbol{\Psi}) \tag{43}$$

Where :

$$\boldsymbol{\Psi} = [\Psi_1, \dots \dots \Psi_s]^T \tag{44}$$

And $\boldsymbol{J}(\boldsymbol{\Psi})$ is the Jacobian matrix:

$$\boldsymbol{J}(\boldsymbol{\Psi}) = \begin{bmatrix} \frac{\partial \Psi_1}{\partial e_{1s}} & \frac{\partial \Psi_1}{\partial e_{2s}} & \cdots & \frac{\partial \Psi_1}{\partial e_{ns}} \\ \vdots & \vdots & \ddots & \vdots \\ \frac{\partial \Psi_s}{\partial e_{1s}} & \frac{\partial \Psi_s}{\partial e_{ns}} & \cdots & \frac{\partial \Phi_s}{\partial e_{ns}} \end{bmatrix} \tag{45}$$

With:

$$\frac{\partial \Psi_k}{\partial e_{js}} = -E_0 \left(1 - \exp(-\frac{t_k}{\tau_{js}}\right) \tag{46}$$

The solution was also addressed using the trust-region-reflective algorithm (implemented in the Matlab function lsqcurvefit [33]) considering the following constraints:

$$e_{js} \geq 0 \quad \forall j \tag{47}$$

And the initial value:

$$e_{js} = 0.001 \tag{48}$$

The terms e_{js} and τ_{js} estimated minimizing Eq (38) are presented in Table 5

Table 5. Parameters of the Prony series from static tests

n_s	τ_{is}	e_{is}
1	317.1245	0.0025
2	995.7220	3.1593e-8
3	3.1264e+3	6.5794e-6
4	9.8165e+3	4.3330e-5
5	3.0822e+4	3.2354e-4

6	9.6777e+4	1.0987e-10
7	3.0386e+5	2.4044e-4
8	9.5409e+5	6.9005e-5
9	2.9957e+6	2.8242e-4
10	9.4060e+6	3.0524e-4

7 DISCUSSION OF THE RESULTS

The relaxation modulus $E(t)$ (in time domain) obtained with Eq. (1) is shown in Fig. 8 together with the curve obtained from DMA tests [19, 20].

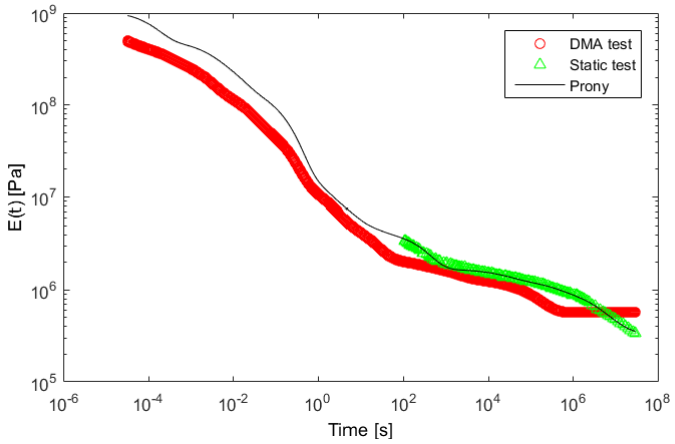

Figure 8. Relaxation modulus $E(t)$ in time domain.

It can be observed that the curve fits the experimental data from static tests quite well. Moreover, the relaxation modulus $E(t)$ obtained with this methodology is sligtly higher than that obtained with a DMA, i.e., the PVB constrained in the laminated glass beams is stiffer than that tested freely at the DMA.

With respect to the frequency domain, the storage modulus $E'(\omega)$ and loss factor $\eta(\omega)$ are presented in Fig. 9. As expected from the static tests, the PVB constrained in the laminated glass beams is stiffer than that tested freely at the DMA, and the estimated curves ($E'(\omega)$ and $\eta(\omega)$) fit the experimental data obtained from the modal tests quite well, although the loss factor has not been considered in the fitting process.

The experimental data were fitted with 19 terms (9 used to fit the frequency domain data and 10 to fit the time domain data), which were defined as optimal to fit the results with a good accuracy. However, when a viscoelastic material is considered in finite element programs, a unique set of Prony terms for the whole mastercurve of the materials is, in general, used [25, 34]. Even the number of Prony terms can be limited, i.e. 13 terms in ABAQUS [25]. This means that if we want to use the curve obtained in this paper in this kind of programs, it would be recommended that the results have to be fitted with a unique Prony's series and, for example, with less terms. However the error increases with decreasing number of terms. This treatment is not very formal from a mathematical point of view, but allows to have the parameters needed in a finite element program.

This approach has been adopted in this paper to illustrate an example. The relaxation curve obtained with 19 terms has been refitted with a new unique Prony series with 12 terms. The parameters e_i and τ_i being presented in Table 6. The relaxation curve with 12 terms and the obtained fitting the whole data with 19 terms are presented in Figures 10.

Table 6. Parameters of the Prony's series using 12 terms ($E_0 = 0.94\ [GPa]$).

e_i	τ_i [s]
3.123615026505222e-04	5.685211253399991e-01
3.107738065983946e-03	1.100135559705064e-01
3.091941806148663e-02	2.271232790353749e-01
3.076225836807449e-01	7.399333082559050e-02
3.060589749853365e+00	1.570125999862382e-02
3.045033139253826e+01	1.400355489128991e-08
3.029555601040031e+02	2.773682891978024e-03
3.014156733296542e+03	1.483992528380668e-04
2.998836136150793e+04	3.361604778877073e-04

2.983593411762730e+05	3.107928821899747e-04
2.968428164314461e+06	4.952656584987844e-04
2.953339999999999e+07	3.576093776560740e-04

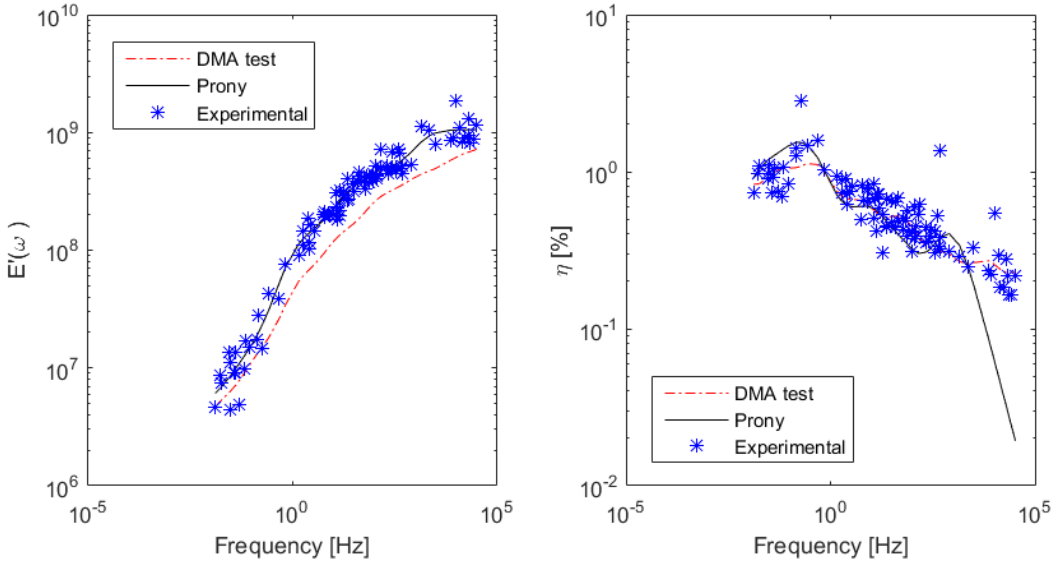

Figure 9. Storage $E'(\omega)$ and loss factor $\eta(\omega)$.

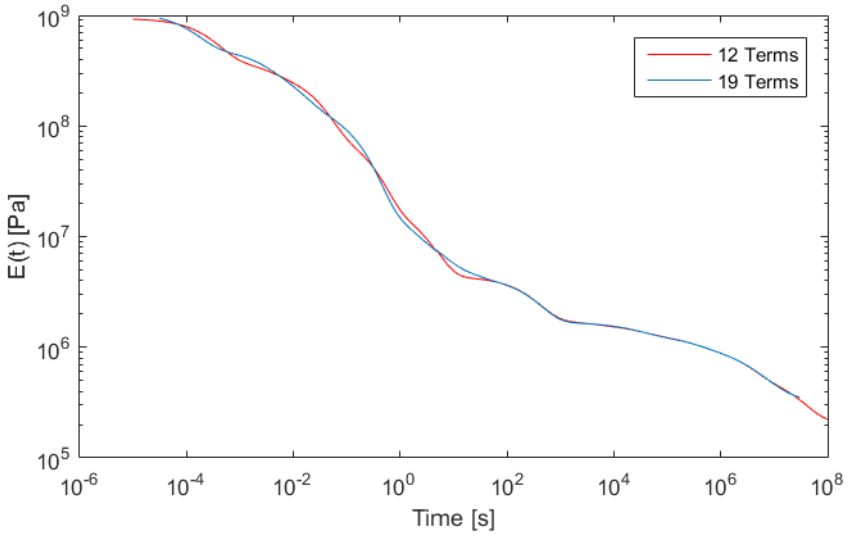

Figure 10. Relaxation modulus $E(t)$ in time Domain with 12 terms.

CONCLUSIONS

Laminated glass elements consists of two or more glass layers and one or more polymeric interlayers, being polyvinil butyral the most common interlayer. In the manufacturing process, the assembly of glass and PVB is laminated together and then placed in an autoclave where it is subject to ramps of pressure and temperature. The process can modify the mechanical properties of PVB, i.e. the PVB constrained in the PVB can exhibit a different behavior to that tested freely in a DMA.

In this paper, it is presented a methodology to determine the mechanical properties of PVB constrained in laminated glass elements, in time (shear modulus $G(t)$) and frequency domain (the complex shear modulus $G^*(\omega)$) from static and modal tests performed on laminated glass beams at different temperatures.

On one hand, several static tests at different temperatures in simply supported laminated glass beams were performed in a climate chamber, from which the shear modulus $G(t)$ was estimated using the model developed by Galuppi and Royer-Carfagni [1]. On the other hand, the complex shear modulus $G^*(\omega)$ was estimated from the modal parameters obtained from experimental modal tests performed on several free-fee laminated glass beams tested at different temperatures and using the model developed by Ross, Kerwin and Ungar (RKU) [5, 6].

The discrete values of $G(t)\ and\ the\ G^*(\omega)$ discrete values were fitted to a Generalized Maxwell model expressed in terms of Prony series. The frequency domain and the time domain data were fitted in separated steps and the joined to obtain a Prony series covering a larger time and frequency ranges. The data from static and dynamic tests performed in laminated glass beams are complementary. The static tests provide information for long times, whereas the modal tests, give information for short times. Moreover, the information from tests at different temperatures in the range $10^oC - 50^oC$ allows to cover the time range from approximately $10^{-5}\ s$ to 10^7 s.

The modulus obtained from the static and the dynamic tests performed on laminated glass beams have been compared with those obtained by testing free PVB specimens in a DMA. The magnitude of the relaxation modulus of PVB obtained from static and modal tests in laminated glass beams is slightly higher than that obtained from testing PVB specimens in tested a DMA, for all the time and frequency range considered in the investigation. This demonstrates that the PVB is affected by the temperature and pressure process in autoclave.

With respect to the loss factor, both types of tests (in laminated glass beams and in free PVB specimens) provide similar results.

REFERENCES

[1] Galuppi, L., and Royer-Carfagni, G.F., Effective Thickness of Laminated Glass Beams: New Expression via a Variational Approach, J Struct Eng, 2012;38:53-67.

[2] Galuppi L and Royer-Carfagni GF. Enhanced Effective Thickness of Multi-Layered Laminated Glass. Compos Part B-Eng, 2014;64:202-213.

[3] Galuppi, L. and Royer-Carfagni, G. The effective thickness of laminated glass plates. J Mech Mater Struct, 2012;7(4):375–400.

[4] Behr, R.A., Minor, J.E., Norville, H.S., Structural behavior of architectural laminated glass. 1993;119(1):202-222.

[5] Kerwin, E.M., Damping of Flexural Waves by a Constrained Viscoelastic Layer, J Acoust Soc Am, 1959;31(7):952-962.

[6] Ross, D., Ungar, E.E., and Kerwin, E.M., Damping of Plate Flexural Vibrations by Means of Viscoelastic Laminate, Structural Damping, ASME, 1959;49-88.

[7] Mead, D.J., and Markus, S., The Forced Vibration of a Three-Layer, Damped Sandwich Beam with Arbitrary Boundary Conditions, J Sound Vib, 1969;10(2):163-175.

[8] Mead D.J., and Markus, S., Loss Factors and Resonant Frequencies of Encastré Damped Sandwich Beam, J Sound Vib, 1970;12(1):99-112.

[9] López-Aenlle, M., Pelayo, F., Frequency Response of Laminated Glass Elements: Analytical Modelling and Effective Thickness, Appl Mech Rev, 2013;65(2), 020802 (13 pages).

[10] Mead, D.J., The damping properties of elastically supported sandwich plates. J Sound Vib. 1972;24(3):275-295.

[11] Tschoegl, N.W.. The Phenomenological theory of linear viscoelastic behaviour. Springer-Verlag, Berlin, 1989.

[12] Lakes, R., Viscoelastic solids. CRC Press, New York, 2009.

[13] Ferry, J.D. Viscoelastic properties of polymers. John Wiley & Sons, New York, 1980.

[14] Phan-Thien, N. On the time–temperature superposition principle of dilute polymer liquids, J Rheol. 1979;23(4):451–456.

[15] Dealy, J., Plazek D., Time-temperature superposition – A users guide. Rheology bulletin, 2009;78(2):16-31.

[16] Honerkamp, J., Weese, J., A note on estimating master curves, Rheologica Acta. 1993;32(1):57-64.

[17] Benninson, S., M.HX, Q. and Davies, P., High-performance laminated glass for structurally efficient glazing. Innovative Light-weight Structures and Sustainable Facades, Hong Kong, May, 2008.

[18] F. Pelayo, M.J. Lamela-Rey, M. Muniz-Calvente, M. López-Aenlle, A. Álvarez-Vázquez, A. Fernández-Canteli. Study of the time-temperature-dependent behaviour of PVB: Application to laminated glass elements. Thin Wall Struct, 2017;119:324-331.

[19] D'Haene, P., Savienau, G., Mechanical properties of laminated safety glass – FEM study, Glass Performance Days, Tampere, Finland, 2007.

[20] López-Aenlle, M., Pelayo, F., Fernández-Canteli, A., García Prieto, M. The effective-thickness concept in laminated-glass elements under static loading. Eng Struct, 56, 1092-1102 (2013).

[21] M. López-Aenlle, F. Pelayo, Static and dynamic effective thickness in five-layered glass plates. Compos Struct, 2019;212:259-270.

[22] Ismael García García, Manuel López Aenlle, Pelayo Fernández Fernández, María Antonia García. Cálculo de desplazamientos en placas de vidrio laminado sometidas a carga estática mediante el concepto de módulo de elasticidad efectivo, Boletín de la Sociedad Española de Cerámica y Vidrio, 2015;54(2):69-76.

[23] López-Aenlle, M., Pelayo, F. Dynamic effective thickness in laminated-glass beams and plates. Compos Part B-Eng, 2014;67:332-347.

[24] Pelayo, F. López-Aenlle M. Natural frequencies and damping ratios of multi-layered laminated glass beams using a dynamic effective thickness. J Sandw Struct Mater (10.1177/1099636217695479), 2017.

[25] Abaqus User's Manual, Dassault Systémes Simulia Corp., Providence, Rhode Island, USA, 2012.

[26] Galuppi, L., Manara, G., and Royer-Carfagni, G. Practical expressions for the design of laminated glass. Compos Part B-Eng, 2013;45(1):1677–1688.

[27] Galuppi, L., and Royer-Carfagni, G.F., The design of laminated glass under time-dependent loading. Int J Mech Sci, 2013;68:67-75.

[28] Jones, D.I.G., Handbook of viscoelastic vibration damping, John Wiley & Sons, Ltd., New York. 2001.

[29] TA Orchestrator User Manual (v7.2.0.4). TA Instruments – Waters LLC, New Castle 2008.

[30] Brincker, R., Ventura, C., Introduction to operational modal analysis. Wiley, 2015.

[31] Williams, M.L., Landel, R.F., Ferry, J., The temperature dependence of relaxation mechanisms in amorphous polymers and other glass-forming liquids. J Am Chem Soc, 1955;77:8701.

[32] Ninomiya, K., Ferry, J.D.: Some approximate equations useful in the phenomenological treatment of linear viscoelastic data. J Colloid Interface Sci. 1959;14:36–48.

[33] MathWorks, MATLAB Documentation R2018b [WWW Document]. URL https://es.mathworks.com/help/matlab/ , 2018.

[34] ANSYS® Academic Research Mechanical, Release 17.1. 2017.

APPENDIX

Geometry and modal parameters of the beams used in the free-free tests.

T(ºC)	Natural frequency (Hz)	Damping ratio (%)	Mode number	L (mm)	b (mm)	H_1 (mm)	t (mm)	H_1 (mm)
11	70.13	0.42	1	1000	100	5.9	0.76	5.8
11	191.9	0.5248	2	1000	100	5.9	0.76	5.8
11	372.1	0.857	3	1000	100	5.9	0.76	5.8
11	606.4	1.25	4	1000	100	5.9	0.76	5.8
11.8	200.9	0.8924	2	1000	100	6	1.14	6
11.8	386	1.3822	3	1000	100	6	1.14	6
11.8	622.2	1.9386	4	1000	100	6	1.14	6
11.9	90.84	0.4038	1	1000	100	7.77	0.76	7.82
11.9	248	0.6854	2	1000	100	7.77	0.76	7.82
11.9	478.9	1.0858	3	1000	100	7.77	0.76	7.82
11.9	775.8	1.5482	4	1000	100	7.77	0.76	7.82
12.4	468.9	0.6924	3	1000	100	7.77	0.38	7.66
12.4	766	1.0018	4	1000	100	7.77	0.38	7.66
16	272.8	1.414	3	1000	100	3.65	1.52	3.77
16	442.3	2.056	4	1000	100	3.65	1.52	3.77
19.9	90.45	0.8594	1	1000	100	7.77	0.76	7.82
19.9	245.2	1.8702	2	1000	100	7.77	0.76	7.82
19.9	470	2.954	3	1000	100	7.77	0.76	7.82
19.9	755.6	4.208	4	1000	100	7.77	0.76	7.82
20	140.3	1.7788	2	1000	100	3.65	1.52	3.77
20	269.2	2.824	3	1000	100	3.65	1.52	3.77

20	433.5	3.898	4	1000	100	3.65	1.52	3.77
20	404.6	2.66	4	1000	100	3.75	0.76	3.7
20.5	69.95	1.2334	1	1000	100	5.8	0.38	5.9
20.5	190	1.7022	2	1000	100	5.8	0.38	5.9
20.5	365.8	2.636	3	1000	100	5.8	0.38	5.9
20.5	591.7	3.744	4	1000	100	5.8	0.38	5.9
21.3	239.5	1.2822	2	1000	100	7.77	0.38	7.66
21.3	463.1	1.9948	3	1000	100	7.77	0.38	7.66
21.3	752.9	2.914	4	1000	100	7.77	0.38	7.66
21.4	189.7	1.896	2	1000	100	5.9	0.76	5.8
21.4	364.7	2.964	3	1000	100	5.9	0.76	5.8
21.4	589.1	4.406	4	1000	100	5.9	0.76	5.8
21.4	73.53	1.4298	1	1000	100	6	1.14	6
21.4	197.7	2.508	2	1000	100	6	1.14	6
21.4	375.8	4.23	3	1000	100	6	1.14	6
21.4	599.6	5.246	4	1000	100	6	1.14	6
25	138.9	3.434	2	1000	100	3.65	1.52	3.77
25	265.2	4.754	3	1000	100	3.65	1.52	3.77
25	422.2	7.582	4	1000	100	3.65	1.52	3.77
25	188.6	2.746	2	1000	100	5.9	0.76	5.8
25	361.4	4.176	3	1000	100	5.9	0.76	5.8
25	584.3	4.976	4	1000	100	5.9	0.76	5.8
25	73.25	1.929	1	1000	100	6	1.14	6
25	195.7	4.036	2	1000	100	6	1.14	6
25	369.1	6.13	3	1000	100	6	1.14	6

25	588.9	6.056	4	1000	100	6	1.14	6
25	238.8	1.6852	2	1000	100	7.77	0.38	7.66
25	461.2	3.046	3	1000	100	7.77	0.38	7.66
25	748	3.868	4	1000	100	7.77	0.38	7.66
25	90.24	1.458	1	1000	100	7.77	0.76	7.82
25	243.8	2.72	2	1000	100	7.77	0.76	7.82
25	465.5	4.152	3	1000	100	7.77	0.76	7.82
25	745.3	5.956	4	1000	100	7.77	0.76	7.82
30	379.8	9.786	4	1000	100	3.75	0.76	3.7
30	253.9	12.146	3	1000	100	3.65	1.52	3.77
30	393.3	10.442	4	1000	100	3.65	1.52	3.77
30	185.9	5.45	2	1000	100	5.9	0.76	5.8
30	353.3	9.376	3	1000	100	5.9	0.76	5.8
30	569.5	8.218	4	1000	100	5.9	0.76	5.8
30	72.85	3.374	1	1000	100	6	1.14	6
30	193.1	6.806	2	1000	100	6	1.14	6
30	359.6	9.096	3	1000	100	6	1.14	6
30	576	6.802	4	1000	100	6	1.14	6
30	236.7	3.314	2	1000	100	7.77	0.38	7.66
30	454.4	5.566	3	1000	100	7.77	0.38	7.66
30	732.6	5.386	4	1000	100	7.77	0.38	7.66
30	89.44	3.048	1	1000	100	7.77	0.76	7.82
30	239.1	5.966	2	1000	100	7.77	0.76	7.82
30	448.6	11.004	3	1000	100	7.77	0.76	7.82
30	713.7	9.18	4	1000	100	7.77	0.76	7.82

35	236.3	17.776	3	1000	100	3.65	1.52	3.77
35	335.3	13.098	3	1000	100	5.9	0.76	5.8
35	183.6	15.224	2	1000	100	6	1.14	6
35	326.5	16.93	3	1000	100	6	1.14	6
35	235.1	4.674	2	1000	100	7.77	0.38	7.66
35	446.9	8.166	3	1000	100	7.77	0.38	7.66
35	718.8	7.19	4	1000	100	7.77	0.38	7.66
35	88.11	6.59	1	1000	100	7.77	0.76	7.82
40	123.6	26.02	2	1000	100	3.65	1.52	3.77
40	67.15	17.994	1	1000	100	6	1.14	6
40	85.48	20.66	1	1000	100	7.77	0.76	7.82
40	219	25.32	2	1000	100	7.77	0.76	7.82
45	104.2	26	2	1000	100	3.75	0.76	3.7
45	41.43	25.08	1	1000	100	3.65	1.52	3.77
45	60.19	16.368	1	1000	100	5.8	0.38	5.9
45	58.53	25.34	1	1000	100	6	1.14	6
45	132.5	29.28	2	1000	100	6	1.14	6
45	205.1	26.18	2	1000	100	7.77	0.38	7.66
50	53.38	20.16	1	1000	100	5.8	0.38	5.9
50	122.2	29.42	2	1000	100	5.8	0.38	5.9
50	213.4	20.16	3	1000	100	5.8	0.38	5.9
50	126.3	35.94	2	1000	100	6	1.14	6
50	74.27	22.14	1	1000	100	7.77	0.38	7.66
50	68.91	27.6	1	1000	100	7.77	0.76	7.82
50	154.4	22.9	2	1000	100	7.77	0.76	7.82

50	274.3	17.406	3	1000	100	7.77	0.76	7.82